Sequence- and Target-Independent Angiogenesis Suppression by siRNA via TLR3

By: Mark E. Kleinman, Kiyoshi Yamada, Atsunobu Takeda, Vasu Chandrasekaran, Miho Nozaki, Judit Z. Baffi, Romulo J. C. Albuquerque, Satoshi Yamasaki, Masahiro Itaya, Yuzhen Pan, Binoy Appukuttan, Daniel Gibbs, Zhenglin Yang, Katalin Karikó, Balamurali K. Ambati, Traci A. Wilgus, Luisa A. DiPietro, Eiji Sakurai, Kang Zhang, Justine R. Smith, Ethan W. Taylor and Jayakrishna Ambati

Abstract:
Clinical trials of small interfering RNA (siRNA) targeting vascular endothelial growth factor-A (*VEGFA*) or its receptor *VEGFR1* (also called *FLT1*), in patients with blinding choroidal neovascularization (CNV) from age-related macular degeneration, are premised on gene silencing by means of intracellular RNA interference (RNAi). We show instead that CNV inhibition is a siRNA-class effect: 21-nucleotide or longer siRNAs targeting non-mammalian genes, non-expressed genes, non-genomic sequences, pro- and anti-angiogenic genes, and RNAi-incompetent siRNAs all suppressed CNV in mice comparably to siRNAs targeting *Vegfa* or *Vegfr1* without off-target RNAi or interferon-α/β activation. Non-targeted (against non-mammalian genes) and targeted (against *Vegfa* or *Vegfr1*) siRNA suppressed CNV via cell-surface toll-like receptor 3 (TLR3), its adaptor TRIF, and induction of interferon-γ and interleukin-12. Non-targeted siRNA suppressed dermal neovascularization in mice as effectively as *Vegfa* siRNA. siRNA-induced inhibition of neovascularization required a minimum length of 21 nucleotides, a bridging necessity in a modelled 2:1 TLR3–RNA complex. Choroidal endothelial cells from people expressing the TLR3 coding variant 412FF were refractory to extracellular siRNA-induced cytotoxicity, facilitating individualized pharmacogenetic therapy. Multiple human endothelial cell types expressed surface TLR3, indicating that generic siRNAs might treat angiogenic disorders that affect 8% of the world's population, and that siRNAs might induce unanticipated vascular or immune effects.
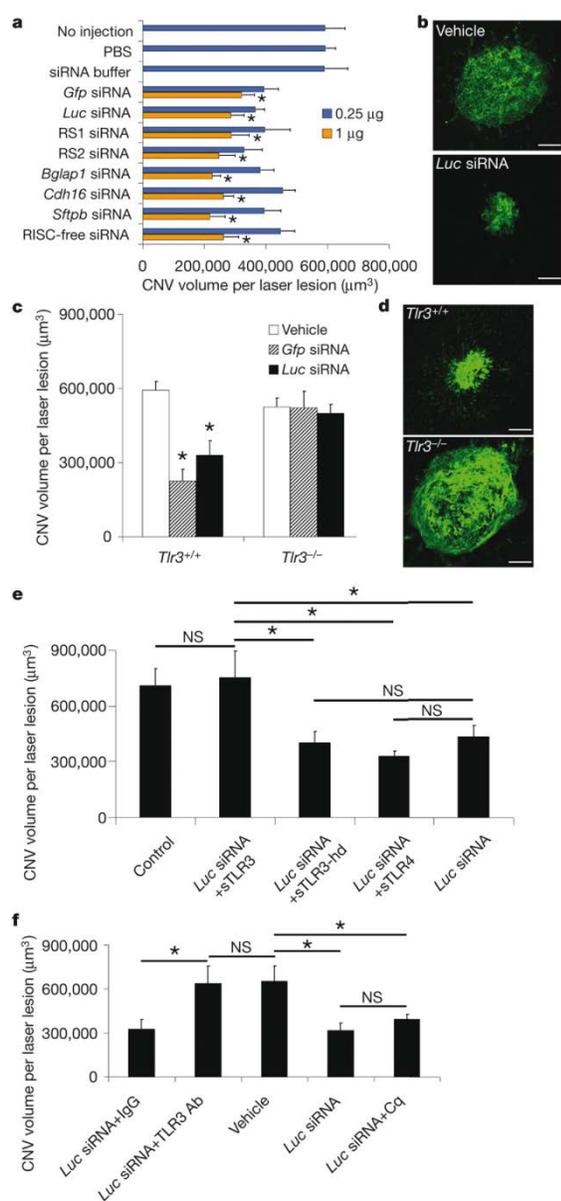
Article:
Therapeutic application of long, double-stranded (ds)RNA-mediated RNAi and sequence-specific gene silencing through RNAi by short synthetic RNA duplexes is challenging because mammalian cells do not uptake 'naked' siRNA (whether chemically modified or not) without cell-permeating entities[1, 2, 3, 4]. To minimize systemic exposure, initial clinical trials of siRNA

were launched using intraocular injection in patients with CNV. CNV, wherein the retina is invaded by choroidal vessels beneath the retinal pigmented epithelium (RPE), is a late stage of age-related macular degeneration that afflicts 30–50 million people globally. The preclinical bases for trials of naked *VEGFA* siRNA (Bevasiranib) or *VEGFR1* siRNA (AGN211745/siRNA-027) were single reports in mice[5, 6] that such siRNAs suppressed laser-injury-induced CNV, a model predictive of efficacy in humans[7, 8]. These findings were interpreted as anomalous examples of local delivery surmounting the impediment to intracellular entry[9, 10, 11]. Instead, we show in two animal models that suppression of neovascularization is a generic property of siRNAs independent of sequence, target and internalization.

SEQUENCE-INDEPENDENT ANGIOGENESIS SUPPRESSION BY siRNA

Numerous synthetic non-targeted 21-nucleotide duplex siRNAs from multiple vendors, when injected into the vitreous humour of wild-type mice, uniformly and dose-dependently suppressed CNV (Fig. 1a, b and Supplementary Fig. 1). siRNAs targeting jellyfish green fluorescent protein (*Gfp*) or firefly luciferase (*Luc*), non-ocular genes *Bglap1* (bone-specific osteocalcin), *Cdh16* (kidney-specific cadherin 16), or *Sftpb* (lung-specific surfactant protein B), or non-genomic random sequences (RS1–6), all suppressed CNV. This stereotypic effect, reproduced independently in the laboratories of J.A. and E.S., cannot be attributed to 'off-target' silencing due to sequence-specific mismatch tolerance[12], nor is it an artefact of intraocular delivery because intraperitoneal administration of serum-stable 2′O-methyl-*Luc*-siRNA suppressed CNV (Supplementary Fig. 2). Furthermore, a siRNA with random sequence and containing proprietary chemical modifications precluding incorporation into RNA-induced silencing complex (RISC) also suppressed CNV (Fig. 1a), whereas a dsDNA analogue of *Luc* siRNA did not (Supplementary Fig. 3). Lipopolysaccharide did not reduce CNV, excluding endotoxin contamination as the source of angio-inhibition; however, nuclease digestion did abolish *Luc*-siRNA-induced CNV suppression. Collectively, these data indicate that angio-inhibition is a siRNA-class effect.

Figure 1: Sequence-independent CNV suppression by siRNA through TLR3.

a, siRNAs targeting *Gfp*, *Luc*, random sequences (RS1, RS2), *Bglap1*, *Cdh16*, or *Sftpb*, and siRNA incapable of RNA-induced silencing (RISC-free), suppressed CNV in wild-type mice. $n = 8$–24; asterisk, $P < 0.05$ compared to no injection, phosphate buffered saline (PBS) and siRNA buffer. **b**, Representative examples of CNV in wild-type eye injected with vehicle (buffer) or *Luc* siRNA (1 μg). **c**, *Gfp* siRNA or *Luc* siRNA suppressed CNV in $Tlr3^{+/+}$ but not $Tlr3^{-/-}$ mice. $n = 16$–18; asterisk, $P < 0.05$ compared to vehicle (buffer). **d**, Representative examples of CNV in *Gfp*-siRNA-injected

(1 µg) *Tlr3*^{+/+} and *Tlr3*^{-/-} eyes. **e**, CNV suppression in wild-type mice by *Luc* siRNA (0.25 µg) was abrogated by soluble TLR3 (sTLR3) but not soluble TLR4 or heat-denatured (hd) soluble TLR3 (all 2 µg). $n = 8$. **f**, CNV suppression in wild-type mice by *Luc* siRNA (1 µg) was abrogated by neutralizing anti-TLR3 antibodies (Ab; 0.2 µl) but not control IgG (0.2 µl) or chloroquine (Cq; 30 ng). $n = 6–8$; asterisk, $P < 0.05$. NS, not significant. Vehicle, buffer. All error bars indicate mean ± s.e.m. Scale bars in **b**, **d** are 100 µm.

SURFACE TLR3 MEDIATES ANTI-ANGIOGENIC ACTIVITY OF siRNA

Consistent with reports that naked siRNAs are not internalized by mammalian cells[1, 2, 3], fluorescein-conjugated *Luc* siRNA did not enter primary human choroidal endothelial cells (CECs) or mouse RPE and CECs (Supplementary Fig. 4). However, fluorescein–*Luc*-siRNA–chol, in which cholesterol is conjugated to the 3′ end to enable uptake[3], was internalized by human and mouse cells, both of which express the mammalian homologue of Sid1, a protein involved in internalizing cholesterol-conjugated siRNAs[13]. We therefore sought a surface receptor mediating siRNA-induced angio-inhibition.

We proposed that siRNAs activate TLR3, a long double-stranded viral RNA sensor[14], to suppress CNV. Indeed, non-targeted siRNAs did not suppress CNV in *Tlr3*^{-/-} mice (Fig. 1c, d). The TLR3 activators polyinosinic:polycytidylic acid (poly(I:C))[14] and *in-vitro*-transcribed long dsRNA[15] suppressed CNV in wild-type mice, whereas the TLR3 non-activators polydeoxyinosinic:polydeoxycytidylic acid (poly(dI:dC))[14] and 2-thiouridine (s2U)-modified *in-vitro*-transcribed dsRNA[15] were ineffective. Poly(I:C) did not suppress CNV in *Tlr3*^{-/-} mice (Supplementary Fig. 5).

Soluble TLR3, but not soluble TLR4 or heat-denatured soluble TLR3, abolished CNV suppression by *Luc* siRNA in wild-type mice (Fig. 1e), suggesting direct interaction of siRNA with TLR3. Fluorescein-conjugated *Luc* siRNA bound wild-type but not *Tlr3*^{-/-} mouse eye sections *in situ* (Supplementary Fig. 6). Using flow cytometry to monitor binding of fluorescein–*Luc* siRNA to the surface of CD31^{+}VEGFR2^{+} mouse choroidal endothelial cells, greater fluorescence was detected on wild-type than *Tlr3*^{-/-} cells (Supplementary Fig. 7). Pre-incubation with soluble TLR3 or competition with poly(I:C) reduced fluorescein–*Luc*-siRNA binding to wild-type mouse CECs. These data extend cell-free system data that 20-nucleotide dsRNAs bind TLR3 (refs 16, 17) and support an *in vivo* siRNA–TLR3 interaction, although we cannot exclude accessory molecules enabling TLR3 activation. However, the only such facilitator reported so far, CD14 (ref. 18), was dispensable because *Luc* siRNA suppressed CNV in *Cd14*^{-/-} mice (Supplementary Fig. 8).

CNV suppression by *Luc* siRNA was blocked by TLR3-neutralizing antibodies (Fig. 1f), suggesting that non-targeted siRNA signalled via surface TLR3. We confirmed *in vivo* surface TLR3 expression on mouse and human CECs by flow cytometry and immunofluorescence (Supplementary Fig. 9). To resolve the locus of TLR3 activation by siRNA, we used chloroquine, which inhibits endosomal TLR3 and TLR9. Chloroquine blocked the increase in CNV induced by CpG oligonucleotide, a TLR9 agonist, but did not prevent CNV suppression by *Luc* siRNA (Fig. 1f and Supplementary Fig. 10). Collectively, these data show that surface, not endosomal, TLR3 mediates extracellular siRNA-induced angio-inhibition.

Non-targeted siRNAs did not suppress CNV in *Trif*[Lps2] mice (Supplementary Fig. 11), which are deficient in signalling induced by TRIF (toll/interleukin (IL)-1-receptor-domain-containing adaptor-inducing interferon-β), the TLR3 adaptor protein[19, 20], confirming TLR3 indispensability. TLR3 signalling can diverge at the level of TRIF through a kinase cascade activating interferon

regulatory factor (IRF)-3 or nuclear factor-κB (NF-κB)[21]. Non-targeted siRNAs suppressed CNV in *Irf3*^{-/-} but not *Nfkb1*^{-/-} mice (Supplementary Fig. 11), suggesting a TRIF–NF-κB cascade.

Duplex siRNAs containing immunostimulatory sequences such as UGUGU[22] or GUCCUUCAA[23] trigger off-target effects via TLR7, a single-stranded RNA sensor. However, none of our siRNAs contained these sequences (Supplementary Table). Also, non-targeted siRNAs suppressed CNV in *Tlr7*^{-/-} mice (Supplementary Fig. 12). Furthermore, 2′*O*-methyl-*Luc*-siRNA suppressed CNV, excluding TLR7 involvement[24].

Although it is improbable that cytosolic dsRNA sensors such as protein kinase R (PKR, encoded by *Prkra*), retinoic-acid-inducible gene 1 (RIG-I), and melanoma differentiation-associated gene 5 (MDA5)[25, 26, 27, 28] are involved in siRNA-mediated angio-inhibition because *Luc* siRNA did not enter cells, we excluded their involvement because siRNA activates PKR when transfected into cells[29]. *Luc* siRNA suppressed CNV in *Prkra*^{-/-} just as in wild-type mice, suggesting that PKR has no involvement (Supplementary Fig. 13). Poly(I:C$_{12}$U), an analogue of poly(I:C) that activates TLR3 but not MDA5 (ref. 30), suppressed CNV in wild-type mice as effectively as poly(I:C) (Supplementary Fig. 5). RIG-I participation is unlikely because *in-vitro*-transcribed dsRNA, which activates RIG-I, and poly(I:C), which does not[25], suppressed CNV equally (Supplementary Fig. 5). Thus, TLR3 seems to be central to siRNA-induced angio-inhibition.

ANTI-ANGIOGENIC INNATE IMMUNITY TRIGGERED BY siRNA

siRNAs sometimes induce type I interferon (IFN)[22, 23, 29, 31, 32, 33]. Although laser injury increased levels of IFN-α and IFN-β (IFN-α/β) in the RPE and choroid, they were not further induced by *Luc* siRNA (Supplementary Fig. 14). *Luc* siRNA suppressed CNV in *Ifnar1*^{-/-} (IFN-α/β receptor null) mice just as in wild-type mice (Fig. 2a). However, type II IFN-γ and IL-12, which are TLR3-inducible, were upregulated by *Luc* siRNA after laser injury (Fig. 2b). Recombinant IFN-γ and IL-12 suppressed CNV in wild-type mice (Fig. 2c), consistent with their anti-angiogenic properties[34]. Both were required for angiogenesis suppression because *Luc* siRNA did not suppress CNV in *Ifng*^{-/-} or *Il12a*^{-/-} mice (Fig. 2a).

Figure 2: CNV suppression by siRNA is mediated by IFN-γ and IL-12.
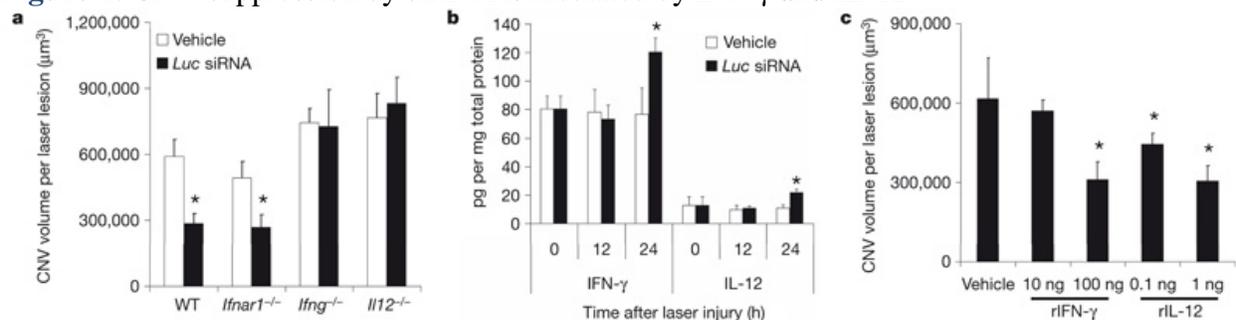
a, *Luc* siRNA (1 μg) suppressed CNV in wild-type and *Ifnar1*^{-/-} mice but not *Ifng*^{-/-} or *Il12*^{-/-} mice. $n = 5$–10. **b**, IFN-γ and IL-12 levels in RPE and choroid at 24 h after laser injury were higher in wild-type mouse eyes injected with *Luc* siRNA (1 μg) compared to vehicle-injected eyes. $n = 12$. **c**, Recombinant IFN-γ or IL-12 reduced CNV in wild-type mice. $n = 8$. Asterisk, $P < 0.05$ compared to vehicle (siRNA buffer). All error bars indicate mean ± s.e.m.

IFN-γ and IL-12 polarization is congruent with TRIF activation being biased towards NF-κB rather than IRF-3. Non-induction of IFN-α/β by synthetic siRNA is consistent with the absence of 5′-triphosphates[33] and the dominant role of MDA5, which is not involved in siRNA-induced

angio-inhibition (Supplementary Fig. 5), in mediating dsRNA-induced IFN-α/β (refs 25, 28). Alternatively, laser injury might have saturated or inhibited IFN-α/β induction.

TARGETED siRNAs ALSO SUPPRESS CNV VIA TLR3

We synthesized a siRNA targeting the same sequence as AGN211745 in *Vegfr1* (*Vegfr1* siRNA, complementary to mouse and human sequences). *Vegfr1* siRNA suppressed CNV in wild-type mice, confirming an earlier report[6], but not in *Tlr3*^{-/-} mice (Fig. 3a), suggesting that it suppressed angiogenesis by means of the class effect, not RNAi. Supportive of this, *Vegfr1* siRNA suppressed CNV as effectively as *Luc* siRNA in mice that lack the tyrosine kinase domain of *Vegfr1* (*Vegfr1(TK)*[-/-] mice, which have no VEGFR1 signalling[35]; Supplementary Fig. 15). Also, *Vegfr1* siRNA did not suppress *Vegfr1* mRNA in the RPE and choroid of *Tlr3*^{-/-} mice (Supplementary Fig. 15). Furthermore, *Vegfr1*-siRNA–chol did not suppress CNV in *Tlr3*^{-/-} mice despite *Vegfr1* knockdown (Fig. 3b and Supplementary Fig. 15), consonant with observations that VEGFR1 does not promote CNV[36].

Figure 3: CNV suppression by targeted siRNAs is mediated by TLR3.
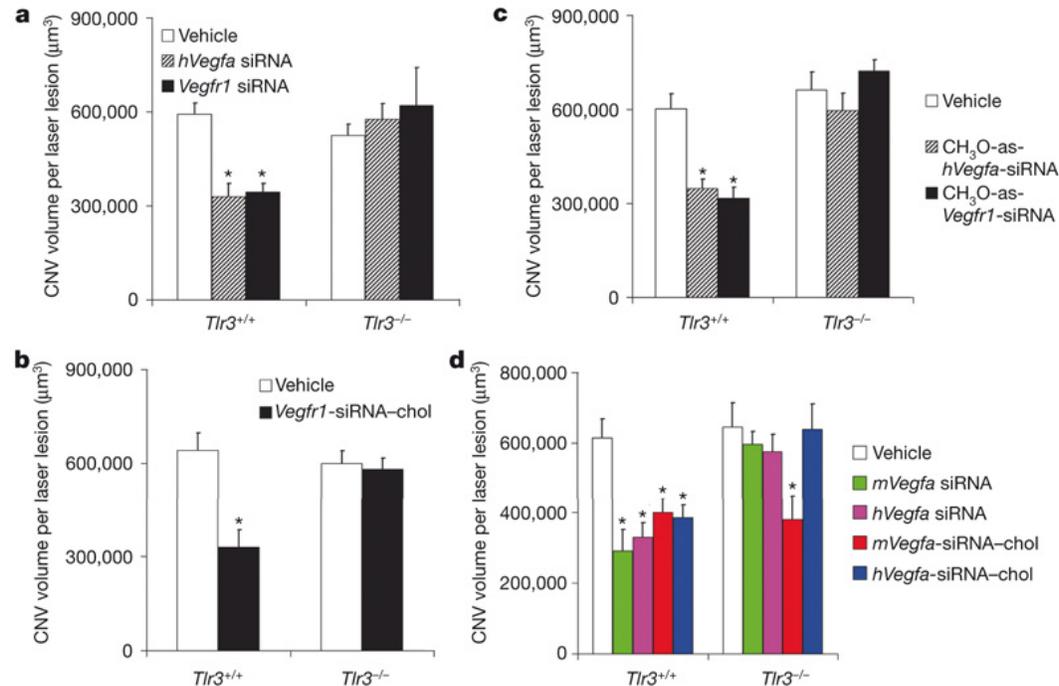
a, *hVegfa* siRNA and *Vegfr1* siRNA suppressed CNV in *Tlr3*^{+/+} but not *Tlr3*^{-/-} mice. **b**, *Vegfr1*-siRNA–chol suppressed CNV in *Tlr3*^{+/+} but not *Tlr3*^{-/-} mice. $n = 5–6$. **c**, *hVegfa* siRNA and *Vegfr1* siRNA, whose anti-sense (as) strands were modified with 5′-methoxy (CH_3O) substitution, preventing incorporation into RISC, suppressed CNV in *Tlr3*^{+/+} but not *Tlr3*^{-/-} mice. $n = 9–14$. **d**, siRNAs targeting mouse (m) or human (h) *Vegfa* reduced CNV in *Tlr3*^{+/+} but not in *Tlr3*^{-/-} mice. *mVegfa*-siRNA–chol and *hVegfa*-siRNA–chol suppressed CNV in *Tlr3*^{+/+} mice; however, *mVegfa*-siRNA–chol but not *hVegfa*-siRNA–chol suppressed CNV in *Tlr3*^{-/-} mice. $n = 8–10$. siRNAs were at 1 μg; asterisk, $P < 0.05$ compared to vehicle (siRNA buffer). All error bars indicate mean ± s.e.m.

CH_3O-as-*Vegfr1* siRNA (containing 5′-methoxy modification of the anti-sense strand, preventing phosphorylation of the 5′-hydroxyl end obligate for RISC incorporation and target cleavage[37, 38], thereby abolishing RNAi activity) suppressed CNV in wild-type mice as effectively as *Vegfr1* siRNA and was ineffective in *Tlr3*^{-/-} mice (Fig. 3c), confirming that *Vegfr1* siRNA suppressed CNV through TLR3, not RNAi.

We also synthesized a siRNA targeting the same sequence as Bevasiranib in human *VEGFA* (*hVegfa* siRNA, complementary to human *VEGFA* but mismatched to mouse *Vegfa* at position 11, critical for functional targeting[39]). Both *hVegfa* siRNA and CH$_3$O-as-*hVegfa*-siRNA suppressed CNV in wild-type but not *Tlr3*$^{-/-}$ mice (Fig. 3a, c), demonstrating that *hVegfa* siRNA also suppresses CNV through TLR3, not RNAi. *hVegfa*-siRNA–chol did not suppress CNV in *Tlr3*$^{-/-}$ mice (Fig. 3d), indicating that this siRNA was incapable of functional targeting even after internalization due to critical nucleotide mismatch with mouse *Vegfa*. However, *mVegfa*-siRNA–chol (complementary to mouse *Vegfa*) suppressed CNV in *Tlr3*$^{-/-}$ mice. As further confirmation of the centrality of this nucleotide, *mVegfa*-siRNA–chol, but not *hVegfa*-siRNA–chol, suppressed *Vegfa* in the RPE and choroid of *Tlr3*$^{-/-}$ mice (Supplementary Fig. 16). Hence, siRNAs unaided by cell permeation cannot execute RNAi.
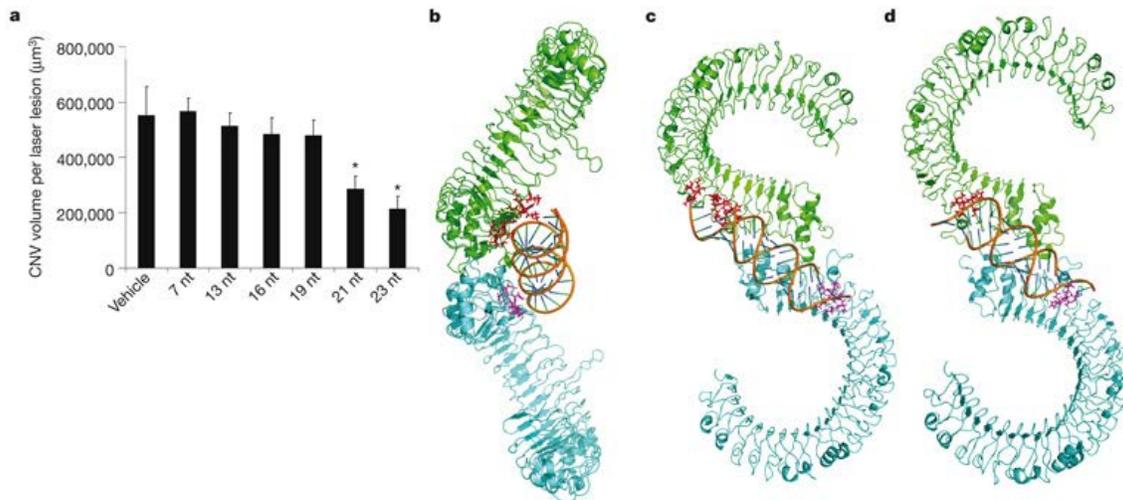
Luc siRNA suppressed CNV ($51 \pm 7\%$) in wild-type mice as effectively as *mVegfa*-siRNA–chol in *Tlr3*$^{-/-}$ mice ($41 \pm 11\%$; Fig. 3d) and anti-VEGFA neutralizing antibodies in wild-type mice ($49 \pm 7\%$; Supplementary Fig. 17), suggesting that TLR3 activation is as effective as VEGFA blockade, the current standard of care. *Luc* siRNA did not affect *Vegfa*, *Vegfr1*, or *Vegfr2* mRNA levels in wild-type mice (Supplementary Fig. 18), so activity seems to be independent of VEGFA pathways. Despite the potential for *mVegfa*-siRNA–chol to activate TLR3 and knockdown *Vegfa* in wild-type mice, there was no angio-inhibitory synergy. This could be attributed to blockade of VEGFA-dependent signalling by IFN-γ (induced by siRNA) and potential crosstalk[40]. Indeed, CNV suppression by *Luc* siRNA or recombinant IFN-γ was not enhanced by co-administration of anti-VEGFA antibodies, consistent with convergence of anti-angiogenic mechanisms (Supplementary Fig. 18). Alternatively, incorporation of *mVegfa*-siRNA–chol into RISC might preclude TLR3 interaction.

Neither *hVegfa* siRNA nor *Vegfr1* siRNA suppressed CNV in *Ifng*$^{-/-}$ or *Il12a*$^{-/-}$ mice (Supplementary Fig. 19), confirming that these targeted siRNAs suppressed CNV via the class effect, not RNAi. As an additional demonstration that siRNA suppresses CNV without target cleavage, *Irf3* siRNA suppressed CNV in *Irf3*$^{-/-}$ mice as effectively as *Luc* siRNA (Supplementary Fig. 20), and *Tlr3* siRNA suppressed CNV in wild-type mice without *Tlr3* knockdown. This class effect was so robust that siRNA targeting *Il12*, which is anti-angiogenic in this model, also suppressed CNV in wild-type but not *Tlr3*$^{-/-}$ mice (Fig. 2c and Supplementary Fig. 21). These data demonstrate that non-targeted and targeted siRNA, without active intracellular delivery, suppressed CNV by means of extracellular TLR3 activation.

MINIMUM LENGTH OF siRNA REQUIRED TO SUPPRESS CNV
The minimum length of dsRNA activating TLR3 *in vivo* is unclear. We found, unlike 21- and 23-nucleotide *Luc* siRNA, 7-, 13-, 16-, or 19-nucleotide versions did not suppress CNV (Fig. 4a). This, coupled with data that longer duplexes such as ~1,000-nucleotide dsRNA and poly(I:C) suppressed CNV (Supplementary Fig. 5), suggest that at least 21 nucleotides are required to activate TLR3. To understand the structural basis of the divergence between 19 and 21 nucleotides, we performed docking simulations between dimeric TLR3, which is required for signalling[17, 41, 42], and dsRNA using crystal structures of TLR3 and 19-nucleotide dsRNA, the latter being shortened or extended as necessary.

Figure 4: Minimum length for TLR3 activation.

a, 21-nucleotide or 23-nucleotide *Luc* siRNA but not truncated versions suppressed CNV in wild-type mice. $n = 8–11$; asterisk, $P < 0.05$ compared to vehicle (buffer); mean ± s.e.m. Equimolar amounts to 1 μg of 21-nucleotide *Luc* siRNA. nt, nucleotide. **b, c**, Orthogonal views of a model of TLR3 ectodomain dimer (green and cyan subunits shown as backbone ribbons) with computer-docked 21-nucleotide dsRNA. Protein modules interact via C-terminal domains to form a highly symmetrical dimer. The model incorporated potential interactions involving a larger set of TLR3 residues considered important in RNA binding (displayed as purple and red side chains on ectodomain subunits); these residues were within 4.5 Å of RNA. **d**, TLR3 dimer with docked 19-nucleotide dsRNA shows proximity to fewer putative RNA-binding residues. Binding of 19-nucleotide dsRNA was less favourable than 21-nucleotide dsRNA ($\Delta E = –308$ kcal mol^{-1}; 95% confidence interval: 261–355; $n = 5$; $P = 0.008$).

Docking of dsRNA of various lengths on a TLR3 ectodomain (ECD) monomer did not clarify the observed minimal length requirement for TLR3 activation because the ECD solenoid is approximately the same width as a single turn of an RNA helix. Therefore, a TLR3 monomer cannot discriminate between dsRNAs greater than about 10 nucleotides in length (data not shown), indicating that TLR3 dimerization is required for the observed length needed for activation. We developed a model of a 2:1 TLR3–dsRNA complex, constrained by these observations or interpretations of known data: (1) active TLR3 involves a specific ECD carboxy terminus dimer, formation of which is stabilized by dsRNA binding[17, 41, 42]; (2) TLR3 residues most critical for RNA binding and receptor activation, H539 and N541 (ref. 41), lie in a region 40–45 Å from the ECD C terminus; (3) dsRNA of 21 nucleotides or longer is required for receptor activation (Fig. 4a), suggesting that a dsRNA of approximately two full helical turns (~50 Å in length) is required to span clusters of RNA-binding residues on two TLR3 monomers.

We proposed that C terminus dimerization of TLR3 ECDs creates a scaffold for RNA binding in which clusters of functional RNA-binding residues are separated by approximately 50 Å. This is possible with significant overlap of the C terminus domains, as would be required for effective dimerization.

Using these constraints, computer docking identified a highly symmetrical C terminus dimer of TLR3 ECD with clusters of RNA-binding residues on the same side of the complex and spaced appropriately (N541 to N541 distance of 50 Å). This dimer was used to dock either 21-nucleotide or 19-nucleotide dsRNA, under the constraint that docked complexes place H539 and N541 on both TLR3 monomers within 5 Å of RNA and be as symmetrical as possible[43]. The resulting 2:1 complexes (Fig. 4b–d) were subjected to short molecular dynamics simulations, from which five time points were sampled and energy minimized, indicating that the 21-nucleotide complex was

approximately 300 kcal mol^{-1} energetically more favourable than the 19-nucleotide complex. This is consistent with experimental results showing a loss in anti-angiogenic activity for dsRNA with fewer than 21-nucleotides (Fig. 4a). Furthermore, 19-nucleotide dsRNA was unable to make contact with as many of the putative RNA-binding residues as 21-nucleotide dsRNA (Fig. 4c, d and Supplementary Figs 22 and 23). The model also allows for binding of longer dsRNAs such as poly(I:C).

We considered possible interactions between dsRNA and an extended set of putative RNA-binding residues including, in addition to H539 and N541, E442, N466, K467, R489, N515, N516, N517, N540 and N572 (refs 17, 44). Compared to 19-nucleotide dsRNA, 21-nucleotide dsRNA made contact (within 4.5 Å) with 80% more side chains. Thus, this model accords with the possibility that these TLR3 residues may contribute in varying degrees to RNA binding, if not actual receptor activation.

This model predicts that although siRNAs shorter than 21 nucleotides cannot bridge functional residues on TLR3 dimers, they can bind just as well as longer siRNAs to TLR3 monomers (Fig. 4d and Supplementary Fig. 23). Indeed, excess 19-nucleotide *Luc* siRNA prevented CNV suppression by 21-nucleotide *Luc* siRNA (Supplementary Fig. 24) in a dose-dependent manner, suggesting that the shorter siRNA can be an inactive competitor by saturating binding sites on TLR3 monomers and interfere with the ability of longer siRNAs to bridge two monomers to form the active dimeric signalling complex. The specificity of this competition was demonstrated by the inability of a dsDNA analogue of 19-nucleotide *Luc* siRNA to interfere with CNV suppression by 21-nucleotide *Luc* siRNA.

CLINICAL IMPLICATIONS
Of the known non-synonymous single-nucleotide polymorphisms (SNPs) in *TLR3*, two (N284I, rs5743316 and L412F, rs3775291) are hypomorphic (associated with a reduction in cell surface expression and functional activation of receptor)[45]. Variance for rs3775291 is prevalent in many populations (minor allele frequency ranges from 0.26 to 0.40 in Asian and European samples) whereas variance for rs5743316 is rare (minor allele frequency <0.01). Therefore we sought to determine whether non-targeted siRNA therapy would have differential effects on patients with different homozygous genotypes at rs3775291 (we did not identify any patients with variance at rs5743316). We scanned a library of primary human CECs isolated from single donors for cells homozygous at rs3775291. To determine the fate of these cells when exposed to extracellular non-targeted siRNA, we assayed their survival in serum-supplemented culture in the presence of serum-stable 2'*O*-methyl-*Luc*-siRNA without transfection reagents. Non-targeted siRNA induced a 38% reduction in survival of 412LL human CECs (consistent with known cytotoxic effects of TLR3 activation), but a 3% increase in that of 412FF human CECs (Supplementary Fig. 25), suggesting that the TLR3 412 genotype is an important determinant of the cell survival response to siRNA and consistent with TLR3-mediated angio-inhibition. However, further confirmation is required to assign differential survival solely to this SNP and to support a role for pharmacogenetic testing of patients before initiating siRNA therapeutics. Apart from CECs, pericytes and leukocytes have critical roles in angiogenesis; defining their contributions awaits the development of tissue-specific TLR3 knockouts.

To determine the potential for siRNA-induced angio-inhibition in other organs, we interrogated human endothelial cells from aorta, dermis, lung and umbilical vein for TLR3 expression. Surface TLR3 was detected on all of these cells (Supplementary Fig. 26). Serum-stable 21-nucleotide 2′O-methyl-*Luc*-siRNA, but not a 7-nucleotide version, suppressed dermal angiogenesis induced by excisional wounding in wild-type mice as effectively as 21-nucleotide 2′O-methyl-*mVegfa*-siRNA (Supplementary Fig. 27), recapitulating the length-dependent anti-angiogenic class effect of siRNA in CNV. The broad angio-inhibitory effect of siRNA and widespread surface expression of TLR3 on endothelial cells suggest that people with the 412LL genotype might be suitable candidates for exploring the anti-angiogenic utility of non-targeted siRNA, whereas targeted cell-permeating siRNA therapies would be better suited for 412FF individuals. Analysing SNPs of genes downstream from *TLR3* might yield refined genomic profiles predictive of response to targeted and non-targeted siRNAs.

DISCUSSION

Our results demonstrate that 21-nucleotide or longer dsRNAs are anti-angiogenic. We show that two investigational siRNAs in clinical trials owe their anti-angiogenic effect in mice not to target knockdown but to TLR3 activation. Our findings support investigations of non-targeted dsRNAs as generic anti-CNV agents as effective as anti-VEGFA antibodies, the current standard of care[8], while avoiding potential neurotoxicity resulting from chronic administration of the latter[46].

Our docking model, although not a high-resolution structure, confirms a potential interaction between 21-nucleotide siRNA and TLR3, and structurally explains TLR3's remarkable length-based discrimination of dsRNAs. Although duplexes shorter than 21 nucleotides did not suppress CNV, our model suggests that they could interact with TLR3 with a free energy of binding below the threshold for dimer stabilization and receptor activation. Such discrimination between interaction and activation, if it exists, might also be attributed to unknown accessory proteins that chaperone siRNA to TLR3. An outstanding question is whether differential binding to monomeric versus active signalling dimeric TLR3 underlies the divergence between 21-nucleotide and shorter siRNAs.

Tlr3^{+/+} and *Tlr3*^{−/−} mice exhibited similar CNV responses in the absence of exogenous dsRNAs, suggesting that TLR3 was dispensable to basal angiogenesis and that endogenous dsRNAs (for example, microRNAs) do not activate TLR3 or influence angiogenesis in this model. Elucidating the discriminants among potential TLR3 ligands will advance understanding of self/non-self immune recognition.

It is tempting to speculate that TLR3 activation and anti-angiogenic dampening by viral transcripts abundant in the human retina–choroid interface (G. S. Hageman, personal communication) might explain why few patients with early age-related macular degeneration undergo the angiogenic switch despite the onslaught of inflammatory stimuli that promote CNV[47]. Similarly, investigations of SNPs in *TLR3* and downstream genes might prove fruitful in revealing new risk-conferring and protective alleles for CNV and atrophic age-related macular degeneration, and predict efficacy of angiogenesis inhibition and susceptibility to adverse vascular effects.

Further studies will determine whether siRNAs, apart from inducing (un)desirable effects on the vasculature, also influence TLR3-mediated antimicrobial immune responses and non-canonical adverse effects of TLR3 activation on pregnancy[48], immune privilege[49] and neuronal growth[50], especially when delivered systemically. Judicious approaches to enhance therapeutic specificity include modifications abrogating TLR3 activation and reducing lengths below 21 nucleotides. Conversely, genomic fingerprinting of patients could hasten angio-inhibitory applications of generic siRNA while avoiding hazards of specific gene targeting.

METHODS SUMMARY

Laser photocoagulation was performed to induce CNV in mice as previously described[36, 47]. CNV volumes were measured by scanning laser confocal microscopy using fluorescein-isothiocyanate-conjugated *Griffonia simplicifolia* isolectin B4 (Vector Laboratories), and compared by hierarchical logistic regression using repeated measures analysis. Chemical siRNA sequences for treatments were purchased from Dharmacon or Ambion, Inc. Sense and anti-sense strands of siRNA were annealed per the manufacturer's instructions, formulated in either sterile siRNA buffer (Dharmacon) or nuclease-free PBS, and injected into the vitreous cavity in a total volume of 1 μl with a 33-gauge Exmire microsyringe (Ito Corporation). The docked complex structures were obtained through rigid-body docking using a modified version of the program FTDock with the X-ray structures of TLR3 ligand-binding domain (Protein Data Bank (PDB) entry 2A0Z) and a 19-nucleotide RNA duplex (PDB entry 1QC0) as the initial structures, the latter being shortened or extended as necessary to generate various lengths of dsRNA with 2-nucleotide overhangs at each end. Final docked 2:1 TLR3–dsRNA complexes were subjected to a short minimization and an implicit solvent molecular dynamics simulation to refine the structures, which were then used for energy calculations. Application of biological information as described above greatly improved the docking results by constraining the sampling space and generating models consistent with the experimental binding data.

REFERENCES

1. Chiu, Y. L., Ali, A., Chu, C. Y., Cao, H. & Rana, T. M. Visualizing a correlation between siRNA localization, cellular uptake, and RNAi in living cells. Chem. Biol. 11, 1165–1175 (2004)
2. Saleh, M. C. *et al.* The endocytic pathway mediates cell entry of dsRNA to induce RNAi silencing. Nature Cell Biol. 8, 793–802 (2006)
3. Soutschek, J. *et al.* Therapeutic silencing of an endogenous gene by systemic administration of modified siRNAs. Nature 432, 173–178 (2004)
4. Song, E. *et al.* Antibody mediated *in vivo* delivery of small interfering RNAs via cell-surface receptors. Nature Biotechnol. 23, 709–717 (2005)
5. Reich, S. J. *et al.* Small interfering RNA (siRNA) targeting VEGF effectively inhibits ocular neovascularization in a mouse model. Mol. Vis. 9, 210–216 (2003)
6. Shen, J. *et al.* Suppression of ocular neovascularization with siRNA targeting VEGF receptor 1. Gene Ther. 13, 225–234 (2006)
7. Krzystolik, M. G. *et al.* Prevention of experimental choroidal neovascularization with intravitreal anti-vascular endothelial growth factor antibody fragment. Arch. Ophthalmol. 120, 338–346 (2002)
8. Rosenfeld, P. J. *et al.* Ranibizumab for neovascular age-related macular degeneration. N. Engl. J. Med. 355, 1419–1431 (2006)

9. Corey, D. R. RNA learns from antisense. Nature Chem. Biol. 3, 8–11 (2007)

10. de Fougerolles, A., Vornlocher, H. P., Maraganore, J. & Lieberman, J. Interfering with disease: a progress report on siRNA-based therapeutics. Nature Rev. Drug Discov. 6, 443–453 (2007)

11. Rana, T. M. Illuminating the silence: understanding the structure and function of small RNAs. Nature Rev. Mol. Cell Biol. 8, 23–36 (2007)

12. Jackson, A. L. *et al.* Expression profiling reveals off-target gene regulation by RNAi. Nature Biotechnol. 21, 635–637 (2003)

13. Wolfrum, C. *et al.* Mechanisms and optimization of *in vivo* delivery of lipophilic siRNAs. Nature Biotechnol. 25, 1149–1157 (2007)

14. Alexopoulou, L., Holt, A. C., Medzhitov, R. & Flavell, R. A. Recognition of double-stranded RNA and activation of NF-κB by Toll-like receptor 3. Nature 413, 732–738 (2001)

15. Kariko, K., Buckstein, M., Ni, H. & Weissman, D. Suppression of RNA recognition by Toll-like receptors: the impact of nucleoside modification and the evolutionary origin of RNA. Immunity 23, 165–175 (2005)

16. Bell, J. K. *et al.* The molecular structure of the Toll-like receptor 3 ligand-binding domain. Proc. Natl Acad. Sci. USA 102, 10976–10980 (2005)

17. Ranjith-Kumar, C. T. *et al.* Biochemical and functional analyses of the human Toll-like receptor 3 ectodomain. J. Biol. Chem. 282, 7668–7678 (2007)

18. Lee, H. K., Dunzendorfer, S., Soldau, K. & Tobias, P. S. Double-stranded RNA-mediated TLR3 activation is enhanced by CD14. Immunity 24, 153–163 (2006)

19. Yamamoto, M. *et al.* Role of adaptor TRIF in the MyD88-independent toll-like receptor signaling pathway. Science 301, 640–643 (2003)

20. Hoebe, K. *et al.* Identification of Lps2 as a key transducer of MyD88-independent TIR signalling. Nature 424, 743–748 (2003)

21. Jiang, Z., Mak, T. W., Sen, G. & Li, X. Toll-like receptor 3-mediated activation of NF-κB and IRF3 diverges at Toll-IL-1 receptor domain-containing adapter inducing IFN-β. Proc. Natl Acad. Sci. USA 101, 3533–3538 (2004)

22. Judge, A. D. *et al.* Sequence-dependent stimulation of the mammalian innate immune response by synthetic siRNA. Nature Biotechnol. 23, 457–462 (2005)

23. Hornung, V. *et al.* Sequence-specific potent induction of IFN-α by short interfering RNA in plasmacytoid dendritic cells through TLR7. Nature Med. 11, 263–270 (2005)

24. Judge, A. D., Bola, G., Lee, A. C. & MacLachlan, I. Design of noninflammatory synthetic siRNA mediating potent gene silencing *in vivo*. Mol. Ther. 13, 494–505 (2006)

25. Kato, H. *et al.* Differential roles of MDA5 and RIG-I helicases in the recognition of RNA viruses. Nature 441, 101–105 (2006)

26. Meurs, E. *et al.* Molecular cloning and characterization of the human double-stranded RNA-activated protein kinase induced by interferon. Cell 62, 379–390 (1990)

27. Yoneyama, M. *et al.* The RNA helicase RIG-I has an essential function in double-stranded RNA-induced innate antiviral responses. Nature Immunol. 5, 730–737 (2004)

28. Gitlin, L. *et al.* Essential role of mda-5 in type I IFN responses to polyriboinosinic:polyribocytidylic acid and encephalomyocarditis picornavirus. Proc. Natl Acad. Sci. USA 103, 8459–8464 (2006)

29. Sledz, C. A., Holko, M., de Veer, M. J., Silverman, R. H. & Williams, B. R. Activation of the interferon system by short-interfering RNAs. Nature Cell Biol. 5, 834–839 (2003)

30. Gowen, B. B. *et al.* TLR3 is essential for the induction of protective immunity against Punta Toro Virus infection by the double-stranded RNA (dsRNA), poly(I:C12U), but not Poly(I:C): differential recognition of synthetic dsRNA molecules. J. Immunol. 178, 5200–5208 (2007)

31. Heidel, J. D., Hu, S., Liu, X. F., Triche, T. J. & Davis, M. E. Lack of interferon response in animals to naked siRNAs. Nature Biotechnol. 22, 1579–1582 (2004)

32. Kariko, K., Bhuyan, P., Capodici, J. & Weissman, D. Small interfering RNAs mediate sequence-independent gene suppression and induce immune activation by signaling through toll-like receptor 3. J. Immunol. 172, 6545–6549 (2004)

33. Kim, D. H. *et al.* Interferon induction by siRNAs and ssRNAs synthesized by phage polymerase. Nature Biotechnol. 22, 321–325 (2004)

34. Voest, E. E. *et al.* Inhibition of angiogenesis *in vivo* by interleukin 12. J. Natl Cancer Inst. 87, 581–586 (1995)

35. Hiratsuka, S., Minowa, O., Kuno, J., Noda, T. & Shibuya, M. Flt-1 lacking the tyrosine kinase domain is sufficient for normal development and angiogenesis in mice. Proc. Natl Acad. Sci. USA 95, 9349–9354 (1998)

36. Nozaki, M. *et al.* Loss of SPARC-mediated VEGFR-1 suppression after injury reveals a novel antiangiogenic activity of VEGF-A. J. Clin. Invest. 116, 422–429 (2006)

37. Nykanen, A., Haley, B. & Zamore, P. D. ATP requirements and small interfering RNA structure in the RNA interference pathway. Cell 107, 309–321 (2001)

38. Martinez, J., Patkaniowska, A., Urlaub, H., Luhrmann, R. & Tuschl, T. Single-stranded antisense siRNAs guide target RNA cleavage in RNAi. Cell 110, 563–574 (2002)

39. Birmingham, A. *et al.* 3' UTR seed matches, but not overall identity, are associated with RNAi off-targets. Nature Methods 3, 199–204 (2006)

40. Battle, T. E., Lynch, R. A. & Frank, D. A. Signal transducer and activator of transcription 1 activation in endothelial cells is a negative regulator of angiogenesis. Cancer Res. 66, 3649–3657 (2006)

41. Bell, J. K., Askins, J., Hall, P. R., Davies, D. R. & Segal, D. M. The dsRNA binding site of human Toll-like receptor 3. Proc. Natl Acad. Sci. USA 103, 8792–8797 (2006)

42. Choe, J., Kelker, M. S. & Wilson, I. A. Crystal structure of human toll-like receptor 3 (TLR3) ectodomain. Science 309, 581–585 (2005)

43. Gay, N. J., Gangloff, M. & Weber, A. N. Toll-like receptors as molecular switches. Nature Rev. Immunol. 6, 693–698 (2006)

44. Takada, E. *et al.* C-terminal LRRs of human Toll-like receptor 3 control receptor dimerization and signal transmission. Mol. Immunol. 44, 3633–3640 (2007)

45. Ranjith-Kumar, C. T. *et al.* Effects of single nucleotide polymorphisms on Toll-like Receptor 3 activity and expression in cultured cells. J. Biol. Chem. 282, 17696–17705 (2007)

46. Nishijima, K. *et al.* Vascular endothelial growth factor-A is a survival factor for retinal neurons and a critical neuroprotectant during the adaptive response to ischemic injury. Am. J. Pathol. 171, 53–67 (2007)

47. Nozaki, M. *et al.* Drusen complement components C3a and C5a promote choroidal neovascularization. Proc. Natl Acad. Sci. USA 103, 2328–2333 (2006)

48. Lin, Y., Liang, Z., Chen, Y. & Zeng, Y. TLR3-involved modulation of pregnancy tolerance in double-stranded RNA-stimulated NOD/SCID mice. J. Immunol. 176, 4147–4154 (2006)

49. Lang, K. S. *et al.* Immunoprivileged status of the liver is controlled by Toll-like receptor 3 signaling. J. Clin. Invest. 116, 2456–2463 (2006)

50. Cameron, J. S. *et al.* Toll-like receptor 3 is a potent negative regulator of axonal growth in mammals. J. Neurosci. 27, 13033–13041 (2007)
51. Muller, U. *et al.* Functional role of type I and type II interferons in antiviral defense. Science 264, 1918–1921 (1994)
52. Sato, M. *et al.* Distinct and essential roles of transcription factors IRF-3 and IRF-7 in response to viruses for IFN-α/β gene induction. Immunity 13, 539–548 (2000)
53. Hemmi, H. *et al.* Small anti-viral compounds activate immune cells via the TLR7 MyD88-dependent signaling pathway. Nature Immunol. 3, 196–200 (2002)
54. Zhang, L. *et al.* Different effects of glucose starvation on expression and stability of VEGF mRNA isoforms in murine ovarian cancer cells. Biochem. Biophys. Res. Commun. 292, 860–868 (2002)
55. Smith, J. R. *et al.* Unique gene expression profiles of donor-matched human retinal and choroidal vascular endothelial cells. Invest. Ophthalmol. Vis. Sci. 48, 2676–2684 (2007)

AUTHOR CONTRIBUTIONS
M.E.K., K.Y., A.T., M.N., J.Z.B., R.J.C.A., S.I., M.I. and E.S. performed CNV experiments. T.A.W. and L.A.D. performed dermal experiments. V.C. and E.W.T. performed modelling simulations. Y.P, B.A. and J.R.S. performed cytotoxicity experiments. D.G., Z.Y. and K.Z. performed genotyping. K.K. provided reagents. J.A. conceived and directed the project, and, with assistance from E.W.T., B.K.A., K.K., B.A. and J.R.S., wrote the paper. All authors had the opportunity to discuss the results and comment on the manuscript.

ONLINE METHODS

Animals

C57BL/6J, $Ifng^{-/-}$, $Il12a^{-/-}$, $Nfkb1^{-/-}$, $Tlr3^{-/-}$, $Tlr3^{+/+}$ and $Trif^{Lps2}$ mice were purchased from The Jackson Laboratory. $Vegfr1(TK)^{-/-}$, $Ifnar1^{-/-}$ (gift from H. W. Virgin), $Irf3^{-/-}$ (gift from T. Taniguchi via M. David), $Prkra^{-/-}$ (gift from R. H. Silverman via G. Luo) and $Tlr7^{-/-}$ (obtained from S. Akira via D. A. Golenbock) mice have been previously described[35, 51, 52, 53].

CNV

Laser photocoagulation (OcuLight GL, IRIDEX) was performed on both eyes of each 6–8-week-old mice to induce CNV as previously described[36, 47]. CNV volumes were measured by scanning laser confocal microscopy (TCS SP, Leica) as reported[36, 47] with 0.5% FITC-conjugated Isolectin B4 (Vector). Results are expressed as mean ± s.e.m. with $P < 0.05$ considered statistically significant.

Drug treatments

siRNAs formulated in siRNA buffer (Dharmacon) or PBS (Sigma-Aldrich), chloroquine (Invivogen), poly(I:C) (Invivogen), poly(dI:dC) (Invivogen), poly(I:C$_{12}$U) (Ampligen; Bioclones), and recombinant soluble mouse TLR3 (R&D Systems), mouse soluble TLR4 (R&D Systems), neutralizing rat antibodies against mouse TLR3 (eBioscience; ref. 48), immunostimulatory CpG oligodeoxynucleotide (ODN), GpC ODN (Invivogen), recombinant IFN-γ (Peprotech), recombinant IL-12 (eBioscience), neutralizing rat antibodies against mouse IL-12 (R&D Systems) and isotype control IgGs (R&D Systems or eBioscience as appropriate) were dissolved in PBS and injected into the vitreous cavity in a total volume of 1 μl. In some experiments, siRNA or vehicle was injected intraperitoneally.

siRNA

Chemical siRNA sequences and modifications are listed in the Supplementary Table. All siRNAs except RS3–RS6 (Ambion) were purchased from Dharmacon.

Protein expression

ELISAs were used to quantify IFN-α/β/γ (PBL) with normalization to total protein (Bio-Rad).

Gene expression

Real-time reverse transcriptase PCR (RT–PCR) was performed (Realplex, Eppendorf) on total mouse RPE and choroid RNA (RNAqueous, Ambion). Primers and Taqman probes for *Vegfa* were described in ref. 54. SYBR green was used for all other assays. Primers for TLR3 were purchased (Superarray), and were custom designed for *Vegfr1* and *Vegfr2* (Supplementary Methods).

Flow cytometry

For surface TLR3 staining, human CECs, isolated as previously reported[55], human aortic endothelial cells (HAECs; gift from E. Reed), human pulmonary artery endothelial cells (HPAECs; Clonetics), human dermal microvascular endothelial cells (HDMECs; Clonetics) and human umbilical vein endothelial cells (HUVECs; Clonetics) cultivated in MCDB-131 media (Gibco) with EGM-2MV (omitting gentamicin, hydrocortisone, Clonetics) were blocked and incubated with PE-conjugated anti-human TLR3 (20 μg ml^{-1}, Imgenex) and FITC-conjugated CD31 (BD Biosciences). For intracellular TLR3 staining, FITC–CD31-labelled cells were fixed and permeabilized with Leucoperm (Serotec) and stained for TLR3 in the presence of 10% mouse serum. PE-conjugated mouse IgGκ1 isotype served as control (BD Biosciences). Samples were analysed on a FACSCalibur (Becton Dickinson) with a minimum of 10,000 events using Kolmogorov–Smirnov statistics.

Suspensions of C57BL/6J RPE and choroid cells (10^6) were isolated 1 day after laser injury and incubated with APC anti-mouse CD31 antibody (20 µg ml^{-1}, BD Biosciences) and PE anti-mouse VEGFR2 antibody (20 µg ml^{-1}; BD Biosciences). For surface TLR3 staining, cells were incubated with anti-mouse TLR3 (10 µg ml^{-1}, R&D Systems) that was pre-conjugated to Alexa Fluor 488 (Invitrogen). For intracellular TLR3 staining, CD31/VEGFR2-labelled cells were subjected to fixation and permeabilization followed by incubation with anti-mouse TLR3 (5 µg ml^{-1}). FITC-conjugated rat IgG2a isotype (BD Biosciences) served as a control.

Fluorescein–siRNA interaction assays
CD31/VEGFR2-labelled RPE and choroid cells (10^6) isolated from C57BL/6J or $Tlr3^{-/-}$ mice 1 day after laser injury were incubated with fluorescein–Luc-siRNA (100 µg ml^{-1}) for 30 min on ice. To determine the specificity Luc siRNA binding to TLR3, fluorescein–Luc-siRNA was pre-incubated with either soluble TLR3, TLR4, poly(I:C), or poly(dI:dC).

Fluorescein–siRNA uptake in mouse RPE and choroid cells
C57BL/6J RPE and choroid cells (10^6) were harvested immediately after laser injury, incubated with 21-nucleotide fluorescein–Luc-siRNA, 21-nucleotide fluorescein–Luc-siRNA–chol (both 100 µg ml^{-1}) or PBS vehicle in phenol-free M199 media (Gibco) plus 10% FBS for 1 h at 37 °C and treated with 150 µl of 0.05% trypsin (Gibco) for 3 min at 37 °C to remove extracellular siRNA.

Immunofluorescent microscopy
Human CECs (10^5) were incubated with 21-nucleotide fluorescein–Luc-siRNA or 21-nucleotide fluorescein–Luc-siRNA–chol (both 100 µg ml^{-1}) for 1 h at 37 °C.

Fluorescein–siRNA binding in mouse RPE and choroid tissue
Frozen sections of C57BL/6J or $Tlr3^{-/-}$ mice prepared 3 days after laser injury and intravitreous injection of Luc siRNA (1 µg) were blocked with 3% BSA and incubated with 21-nucleotide fluorescein–Luc-siRNA (10 µg ml^{-1}) for 1 h at 37 °C. Slides were fixed with 4% PFA, blocked in 10% normal rabbit serum, incubated with rabbit anti-FITC antibody (1:100, Zymed) overnight at 4 °C followed by anti-rabbit Alexa Fluor 488 (1:200, Invitrogen).

TLR3 localization
C57BL/6J mouse eye sections (10 µm) were fixed in ice-cold acetone for 10 min at 4 °C, blocked, and incubated with rabbit anti-mouse TLR3 (1:50, Imgenex) overnight at 4 °C followed by Alexa Fluor 594 goat anti-rabbit IgG (1:200, Invitrogen) For co-labelling of CECs, sections were incubated with rat anti-mouse CD31 (1:50, BD Biosciences) followed by goat anti-rat IgG conjugated to Alexa Fluor 488 (1:200). Human CECs, isolated from donated eyes using anti-CD31 antibody-coated magnetic beads (BD Biosciences and Invitrogen, respectively) as previously described[55], were grown in chamber slides (Lab-Tek). For surface staining, cells were blocked with PBS-1% BSA and incubated with mouse anti-human TLR3 (20 µg ml^{-1}, eBioscience). For surface membrane co-localization, cells were stained with rabbit anti-CD46 (1:50, Santa Cruz). Goat anti-mouse Alexa Fluor 488 and donkey anti-rabbit Cy3 (both 1:400) were used as secondary antibodies. Mouse IgGκ1 isotype antibody (20 µg ml^{-1}, eBioscience) served as a control.